Computers and Electronics in Agriculture 202 (2022) 107381

Contents lists available at ScienceDirect

Computers and Electronics in Agriculture

journal homepage: www.elsevier.com/locate/compag

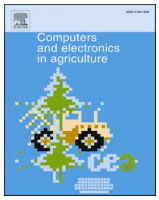

Use of ultrasound anemometers to study the influence of air currents generated by a sprayer with an electronic control airflow system on foliar coverage. Effect of droplet size

Bernat Salas [a], Ramón Salcedo [a], Paula Ortega [a], Marco Grella [b], Emilio Gil [a,*]

[a] Universitat Politècnica de Catalunya, Department of Agri Food Engineering and Biotechnology (DEAB), Esteve Terradas 8, Campus del, Baix, Llobregat D4, 08860 Castelldefels, Barcelona, Spain
[b] Department of Agricultural, Forest and Food Sciences (DiSAFA), University of Torino (UNITO), Largo Paolo, Braccini, 2, 10095 Grugliasco (TO), Italy

ARTICLE INFO

Keywords:
Apple trees
Air velocity
Turbulence intensity
Axial fan
Droplet size

ABSTRACT

Air assistance and droplet's characteristics influence on the pesticide deposit and its distribution over the intended target during the spray application process. The present research work is focused on the characterization of the leaf coverage and the overall spray distribution within the whole canopy by combining different settings of air assistance with different nozzles, generating different droplet's sizes. A new designed air-assisted orchard sprayer was tested, presenting a wireless remote-regulation system to control the airflow rate from the fan by adjusting the blade pitch. In this way, five airflow rates were obtained by combining the gearbox position and the blade pitch. For each one of these five air settings, three droplet sizes (F-Fine, M−Medium, and C-Coarse) were combined and evaluated over a set of artificial apple trees. The evaluation was divided in two parts: a) a whole characterization of the airstream generated by the five air settings was performed for the two sprayer's sides using a 3D-ultrasonic anemometer and placing the sprayer in front of the artificial trees and b) a coverage tests for each nozzle-air settings combination by using water sensitive papers (WSP) placed at different heights and depths evenly distributed across the canopy, the WSP's were analyzed by a processing image software. The results demonstrated that ultrasonic anemometers were helpful to characterize the airstream and to analyze its effect on leaf coverage. Experimental data showed that a higher airflow rate and a larger droplet size generated a more homogeneous coverage on both sides of the sprayer. In this line, the turbulence intensity data suggest that larger variations in the air velocities increase the drag coefficient. Which meant that the canopy resistance to the air stream increased. In addition, an increase of turbulence intensity generated higher spray coverage. Therefore, a higher turbulence intensity did not imply a better spray coverage. It was also observed that the droplet size was critical on regulating the airflow influence on spray coverage. Coarse droplet size did not present any relation with the airflow changes. While the fine droplet size presented a high dependency on airflow conditions.

1. Introduction

In the last decades, modern agriculture aimed to use the Plant Protection Products (PPPs) in a more sustainable way for both environment and human safety. To achieve this objective, the Sustainable Use of Pesticides 2009/128/EC (EC, 2009) was published to establish a regulatory framework in the EU. More recently, the European Green Deal (EC, 2019) stablished several strategies, like the "Farm to Fork" and Biodiversity Strategy (EC, 2020a,b). These strategies aimed to balance the food systems and biodiversity, in such a way that protects the human health as well as increase the EU's competitiveness and resilience. One of the proposed actions established at the Farm to Fork strategy to achieve this objective, is minimizing the use and the risk of PPPs, such as a 50 % reduction of agrochemical products. For this reason, it is necessary to investigate current pesticide application systems in order to increase treatment efficiency, as well as the development of new spraying techniques. In this sense, numerous European projects are being promoted and financed. One of them is the Optimised Pest Integrated Management international project (OPTIMA) (https://optima-h2020.eu), supported by the European Union's Horizon 2020, aimed to develop new sprayers generating a more efficient, safe and sustainable application of the pesticides regarding the environment.

* Corresponding author.
E-mail address: emilio.gil@upc.edu (E. Gil).

https://doi.org/10.1016/j.compag.2022.107381
Received 22 June 2022; Received in revised form 5 September 2022; Accepted 6 September 2022
Available online 23 September 2022

The work of continuous research is justified by the complexity that the treatments entail. Spray application of pesticides is a process with a high environmental risk (Schäfer et al., 2019), but at the same time indispensable nowadays in agriculture (Tilman et al., 2011). It can cause damage on non-target organisms, contaminate water resources (Sultana et al., 2005, Gaona et al., 2019), generate residues in food commodities (Benbrook and Baker, 2014), or create adverse effects on human health (Sankhla, 2018). In the case of specialty crops (orchards trees, vineyard, almonds, olive trees, citrus…), the application of phytosanitary products can pose even more challenging, because, in general, the pesticide is sprayed side-away normally, and assisted by an airflow trying to reach high parts of the trees while guaranteeing penetration into the target canopy (Salcedo et al., 2017, Hong et al., 2018).

The traditional pesticide application equipment in orchards is the airblast sprayers. These sprayers require several adjustments such as the pesticide dose (Xun et al., 2022), the spray liquid distribution (Gil et al., 2013), the forward speed (Van de Zande et al., 2005) or the air settings (Fox et al., 2008). These sprayers generate an airflow that helps on droplets transport and on to achieve a good penetration within the canopy. This same airflow, which pushes the droplets towards the vertical vegetation target, adds an even higher environmental hazard component (Grella et al., 2017, Garcerá et al., 2017). The extra boost provided by the airflow of the airblast sprayer, can drive the droplets above the canopy or even beyond the orchard (Baldoin et al., 2001), increasing the risk of spray drift (ISO, 2005). A fraction of the sprayed volume could reach out other crops, populated areas, water resources, or directly to the atmosphere (Carvalho, 2017).

Concerning the airflow rate, it is well known the difficulties encountered to generate a uniform air distribution with conventional orchard sprayers, with the corresponding influence of the canopies on the sprayed droplets behavior (Da Silva et al., 2006, Delele et al., 2007). To adjust the airflow, the fan design (Dekeyser et al., 2013, Balsari et al., 2017), the rotational speed (Garcerá et al., 2022) and the blade pitch should be set according to the canopy structure (Salcedo et al., 2021, Grella et al., 2022a). Therefore, due to the fan influence on the spray applications efficiency, it is necessary the arrangement of a holistic view of the whole problem (Musiu et al., 2019). The airflow physical behavior should be considered in parallel to its influence on the spray distribution and add new aspects as the interaction between droplet spectra from the nozzle selected and the airflow rate.

The droplet size is another relevant factor of the pesticide treatments, as it is closely related to airborne drift losses (Nuyttens et al., 2007a, Gil et al., 2014). Small droplets can remain longer into airborne with high risk to be carried away by crosswind (Hilz et al., 2013). Furthermore, variations in airflow rate will directly interact with the spray distribution (Miranda-Fuentes et al., 2018, García-Ramos et al., 2018) and, consequently, to the efficiency of the process. Several authors focused their research on the use of air-induction nozzles to reduce the spray drift (Balsari et al., 2017, McCoy et al., 2022), while ensuring the biological efficacy (Doruchowski et al., 2017). This type of nozzle consists of a pre-orifice chamber, that mix the liquid with air and increase droplet size to reduce spray drift (Ferguson et al., 2015). In any case, it is essential to know the droplet size to be used. For this reason, nozzle manufacturers usually report the particle size range based on the classifications proposed by international standards for the classification of nozzles (ISO, 2018, ASABE, 2020).

It is important to characterize how droplets reaches and penetrates the canopy, and which are the main factors affecting the exceeding amount of pesticide from the intended target. Some previous research considered the airflow influence on spray quality (Marucco et al., 2008, Miranda-Fuentes et al., 2015a,b, Pascuzzi et al., 2017, Xiahou et al., 2020). However, these researches only focused on the air velocities, while not considering other important aspects, such us the turbulence intensity (Salcedo et al., 2015 and 2021). Taking into account the circumstance that currently many sprayer manufacturers offer the possibility of modifying several parameters of the fan, such as the gearbox position or the blade pitch, it could be used to study how the turbulence currents of the variable air assistance systems affect the uniformity and penetration of product distribution according to the nozzle size used.

The objective of the present work was to study the influence of the air fan configuration of an airblast sprayer with an air system electronically regulated, on the air stream characteristics and leaf coverage, during a spray application in fruit trees by considering the nozzle size classification. This work is part of the studies carried out within the OPTIMA project for the apple case.

2. Materials and methods

2.1. Sprayer characteristics

The sprayer used for trial purposes was a commercial airblast sprayer Fede Inverter Qi 9.0 (FEDE SL, Cheste, Spain) provided with a tank of 2,000 L of nominal capacity (Fig. 1). The sprayer had a 900 mm diameter reverse axial-fan, suctioning air from a 0.4 m length zone, placed in front of a tower-shape air conveyor. The fan was featured by ten blades rotating anticlockwise from a rear point of view of the sprayer. There were also ten additional deflectors fixed in the air inlet of the fan. These deflectors were to enforce the incoming air stream to enter the fan in the most homogeneous way possible, and therefore improving the subsequent symmetrical distribution of the outgoing air current on both sides of the sprayer. In addition, the air conveyor helps on driving the airflow more homogeneously towards the canopy at different heights. The tower-shaped air conveyor was composed by two metal plates of 1.60 m height, 1.20 m width, and separated between them 0.14 m. It was also equipped with three deflectors per side to better conduct the air currents on the top part of the canopy, and possibly minimize the spray volume fraction directly conveyed by the airflow above the target. Two of them were placed internally on the air conveyor, just at the airflow discharge outlet zone, at 0.80 m and 1.00 m from the bottom. They were fixed with an orientation of 60° respect to the ground. The remaining deflector was placed externally on the top of the air conveyor, orientated at 30°, according to ISO 22,522 standard (ISO, 2007). Ten double nozzle holders per sprayer side were mounted at the edge of the air conveyor to adjust the nozzle height and orientation. The distance between nozzles was manually fixed at 167 mm. The upper nozzle holder was sticked on the external top deflector so that the nozzle pitch was parallel to the deflector.

Furthermore, the sprayer was equipped with the H3O® electronic control system (Berger et al., 2019). Substantially, this technology enables to monitor and modify the spray application parameters directly from the tractor cab by means of a tablet connected to the sprayer via Wi-Fi. The variables displayed by the tablet were obtained from different measuring sensors in real time, such as speedometer, pressure sensors, and flowmeters. This information could be used to take the adequate decisions during the applications. One of the main capabilities of H3O® smart system is the possibility to automatically vary the fan airflow characteristics (Salcedo et al., 2021). When the Power Take Off (PTO) is stopped, the operator can remotely change the blade pitch in the range of 20° and 35°, accounting for the minimum and maximum blade pitch settings, at 5° intervals (Fig. 2.). The larger the blade pitch, the higher airflow rate. The sprayer fan was also provided of two fan gear-box speeds that can be manually selected, namely short and large. These gear-box positions define the transmission power/torque relation between the tractor engine and the fan, being this force transmitted by the PTO. The factors of PTO to fan were 1/3.8 and 1/4.1 for short and large positions, respectively.

2.2. Sprayer settings

To analyze the influence of the droplet size spectra and air assistance on the spray coverage, fifteen working configurations were tested. Five fan settings and three nozzle settings accounting for three different

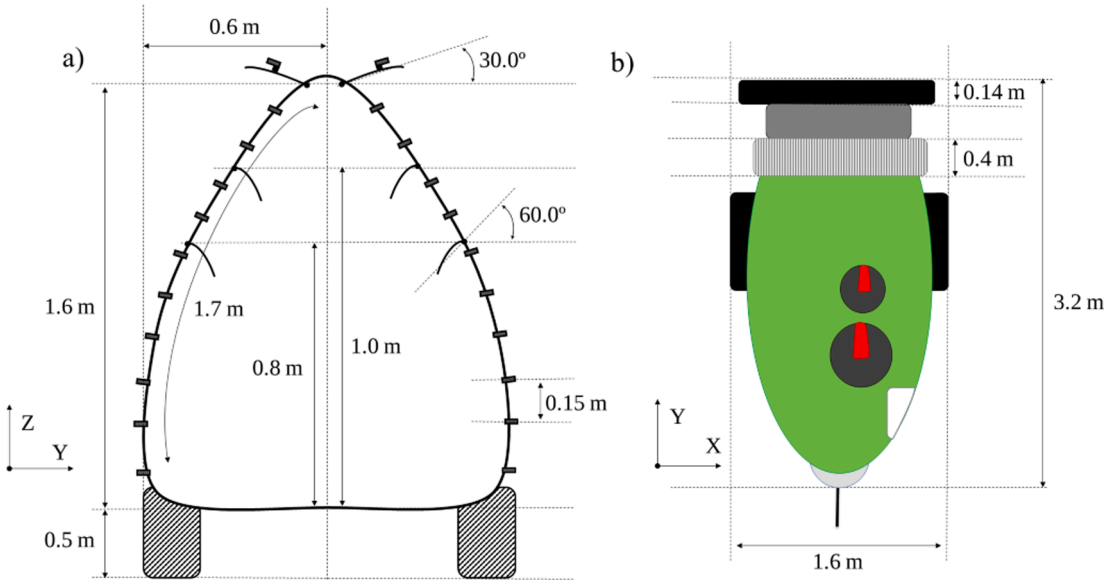

Fig. 1. Tower-shaped axial fan sprayer Fede Inverter Qi 9.0 used for the trials: (a) schematic view from a rear point of view and (b) top view.

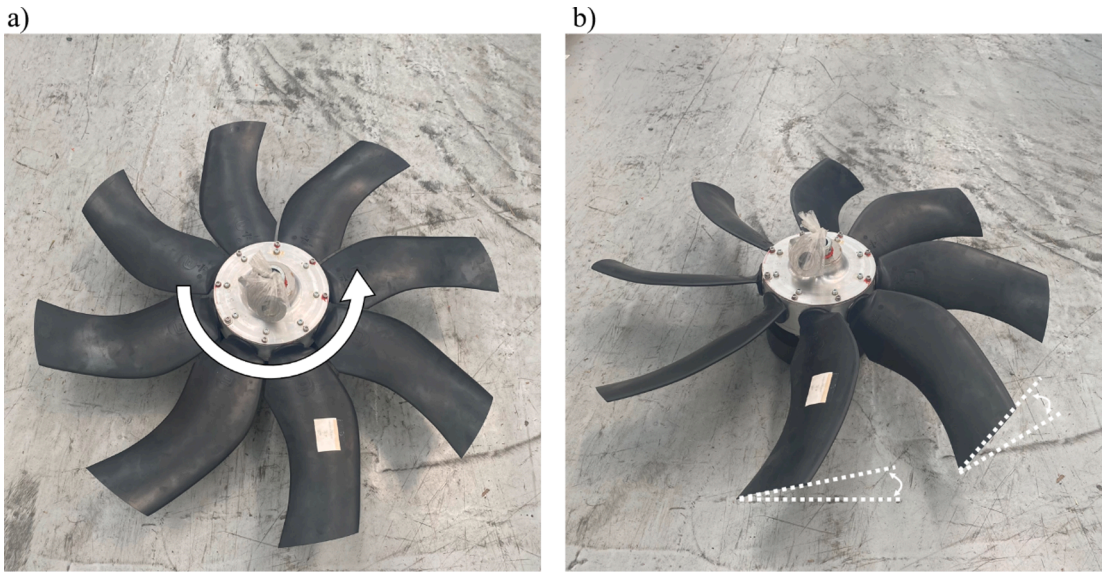

Fig. 2. Fan with a) the blades configured perpendicular (0°) to its rotating sense and b) the blades configured at a defined pitch angle between 20° and 35°.

droplet size spectra generated were combined.

On one side, the fan settings selected were obtained by combining two gearbox positions (large and short) with the minimum (20°) and maximum (35°) blade pitches, respectively. In addition, the manufacturer's air adjustment recommendation at full growth stage (large 30°) was also considered. On the other side, the main characteristics of the three nozzle combinations used in this study are presented in Table 1. The trials to determine the droplet size spectra were performed at the Spray Technology Laboratory of Flanders Research Institute for Agriculture, Fisheries and Food (ILVO, Merelbeke, Belgium), using a Phase Doppler Particle Analyser (PDPA) laser-based measuring set-up. These experiments were within the activities of OPTIMA project. More details about the measuring system and methodology are given by Nuyttens et al., 2007b. To classify the disc-core nozzles into the corresponding

Table 1
Main characteristics and operative parameters of nozzles used for the trials.

Nozzle type	Droplet size classification	VMD (μm)	Pressure (MPa)	Nozzle N°	Unitary flow rate (L min^{-1})
D3-DC25	F	174	1.18	20	1.41
D3-DC35		183		2	2.17
IDK9002	M	333	1.09	20	1.52
IDK9003	C	386	0.49	20	1.52

categories the ASABE Standard S572.3 (ASABE, 2020) were used. The droplet sizes were classified such as fine (F), medium (M), and coarse (C).

For the fine droplet category, eleven Teejet disc-core hollow-cone nozzles (Spraying Systems Co., Teejet Technologies, Illinois, USA) were used: ten D3-DC25 nozzles were installed from the first nozzle holder placed on the bottom part of the air conveyor up to the tenth nozzle holder, while one D3-DC35 nozzle were mounted on the top nozzle holder placed on the top-deflector. For the medium classification, ten IDK9002 Lechler air-induction nozzles (Lechler GmbH, Metzingen, Germany) per sprayer side with the top nozzle on the deflector not activated. For the coarse size, ten IDK 9003 Lechler air-induction nozzles were mounted per each side of the sprayer, with the highest nozzle closed.

To simulate a real application, it was assumed a conventional application rate in apple trees of 900 L ha^{-1} (Xun et al., 2022). The distance between tree rows was 4.0 m. The travel speed of the sprayer was 5.0 km h^{-1} coinciding with the most typical forward speed used by the orchard farmers (Marucco et al., 2019). In all cases the tractor Power Take-Off (PTO) was set at 480 rpm as recommended by the manufacturer.

2.3. Artificial canopy

Four artificial apple trees were developed to carry out trials under controlled conditions avoiding the variability of canopy architecture and characteristics (Gil et al., 2020). Several researchers used artificial canopy in previous studies because this solution allows saving time-consumption as well as performing trials out of seasons (Dekeyser et al., 2014, Zhou et al., 2015, Salcedo et al., 2019). The artificial trees were *ad hoc* designed considering the physical characteristic in the apple orchard plots used for further field trials in the ambit of OPTIMA project.

The artificial trees built (Fig. 3a) were featured by 0.86 m width, 1.64 m length and 3.50 m height. The main trunk had two nodes, the lowest one was placed at 0.65 m height above the ground and the upper one at 2.15 m height. In the lower node four primary branches of 1.25 m length were inserted with an orientation of 45° respect to the ground. In the highest node a second set of wood primary branches of 1.0 m long were inserted using the same angle (45°). This tree structure was provided of 140 holes on specific positions of the main trunk and ramifications, allowing to add or remove secondary branches that defined the tree density. Secondary branches were made with plastic, and they were featured by 42 leaves each one. To measure the leaf surface, ten plastic branches were defoliated and scanned with a LI 3100C electronic planimeter (LI-COR, Lincoln, USA) using the methodology exposed by Gil et al., 2011. The mean leaf area was 22.7 cm^2 for every single branch; therefore, the whole canopy could provide a leaf area from 0.0 m^2 to 13.3 m^2 (full-density mode). For the tests performed in this study, the artificial trees were set at full-density mode. To obtain a volume that fitted the real canopy, it was modelized by two rectangular frustums (the bottom was inverted) and one rectangular cuboid in between (Fig. 3b). Measuring the correspondent canopy dimensions, the average volume was 2.5 m^3 per tree.

2.4. Air currents measurement

2.4.1. Airflow rate

The airflow rate was estimated at the sprayer outlet placing a Meteo Digit I 2D-propeller anemometer (Lambrecht meteo GmbH, Göttingen, Germany) to measure the air velocities. Each sprayer side had a surface of 1700 mm × 140 mm. Considering the total area as the sum of both sprayer sides outlets, ISO 9898 standard (ISO, 2000) recommends a maximum area covered by each sample point of 100.0 cm^2, and at least 40 measurement points. Therefore, the total outlet sampling grid was composed by 66 measuring points, 33 per sprayer side (11 points in height and 3 in width) (Fig. 4). Each measuring point accounts for an area of 155.0 mm × 47.0 mm. Two replications were performed, placing the anemometer at the center of the corresponding sub-area, and perpendicular to the normal surface vector. In each sampling position data was recorded at a frequency of 1 Hz during 30 s.

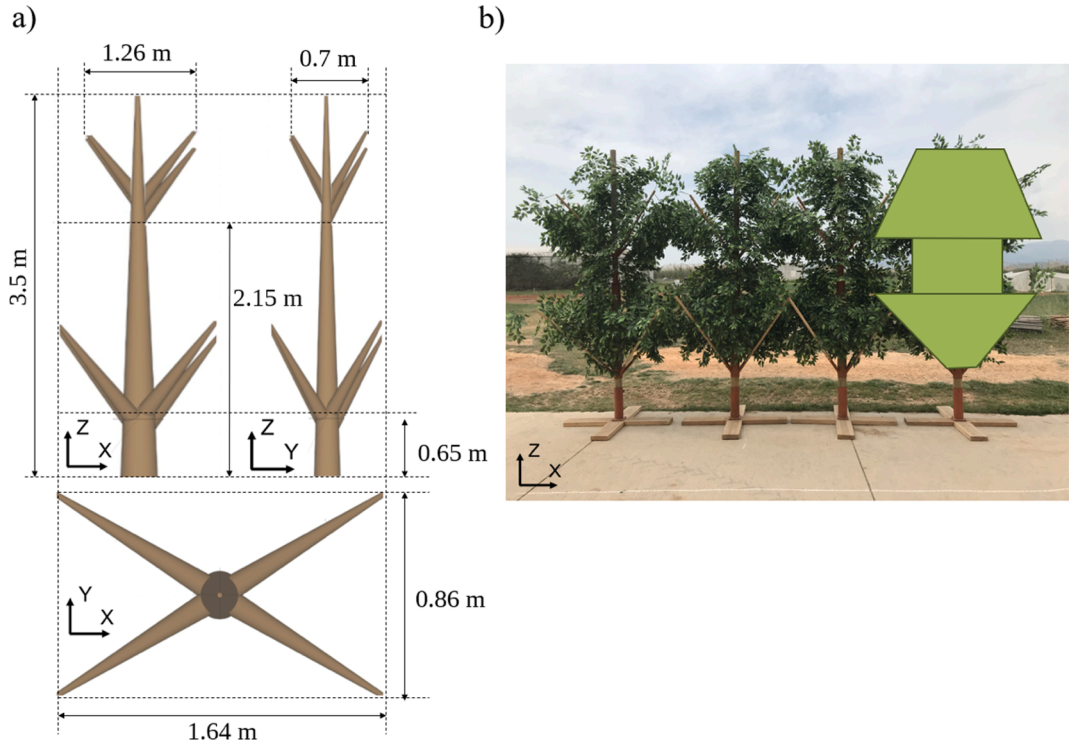

Fig. 3. (a) Model of the three perspectives from the artificial tree structure, without plastic branches, and (b) the four artificial trees in a row, in the full-density mode and the scheme of the canopy volume approximation.

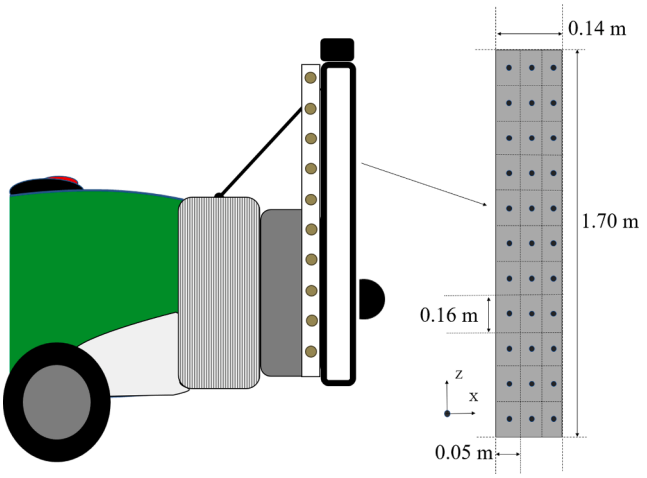

Fig. 4. Schematic view of the sampling grid procedure. The outlet fan was divided in 33 sub-areas per side, accomplishing the measurement procedure established at ISO 9898 standard (ISO, 2000).

2.4.2. Airflow behavior before and after the canopy.

During an orchard application, the canopy presents an aerodynamic resistance (drag) to the airflow (Da Silva et al., 2006), increasing the turbulence around the tree. For this reason, the air velocities generated by each fan configuration were measured before and after the canopy. The measurement procedure for the air velocities was based on the methodology proposed by Salcedo et al., 2019. A Windmaster 3D-ultrasonic anemometer (Gill Instruments, Meteorological technology, Hampshire, UK) was used to register the air velocities (Fig. 5a). This sensor measured the three instantaneous air velocities (u_x, u_y, u_z) in an interval between 0.0 m s^{-1} and 50.0 m s^{-1} with an accuracy of 1.5 %, and at a frequency of 10.0 Hz. It had an air direction range from 0.0° to 359.0° with a resolution of 0.1°. A lifting steel device (Fig. 5b), with a manual control and a maximum height of 5.0 m, was used to hold the anemometer in a fix position at any measuring point. During the trials the sprayer was maintained static in front of the artificial tree. The fan outlet was aligned with the tree axis (Fig. 5c).

Fig. 6a shows a schematic view of the trees and the relative sprayer position during the trials. The positive *Z* semi-axis was perpendicular to the ground (pointing the atmosphere); the positive *Y* semi-axis was perpendicular to the forward driving direction and following the main air currents to the trees; and the positive *X* semi-axis was parallel to the sprayer towards the tractor. The sprayer was placed at 2.0 m from the canopy axis. The distance between the external part of the canopy and the fan outlet was 0.9 m. The air outlet was aligned with the center of the target apple tree at $X = 0.0$ cm, coinciding with the plane *Y-Z*. The air velocities were measured at two positions along the plane $X = 0.0$ cm per each sprayer side, denoted as '*P*1′ and '*P*2′. *P*1 was placed between the canopy and the sprayer, whereas *P*2 was placed behind the canopy. Both were located 0.8 m from the center of the trunk but in opposite directions (Fig. 6a). The separation between *P*1 and the air outlet section was 0.6 m. From each measuring position, air velocities were collected on 19 heights, from 0.4 m above the ground up to 4.0 m high, at intervals of 0.2 m (Fig. 6b). At each height, air velocities were registered during 1.0 min at a frequency of 10.0 Hz, given a total of 600 samples per height.

2.5. Characterization of spray distribution on the canopy

Spray coverage within the whole canopy structure was evaluated for the fifteen working configurations, resulted by combining the five fan settings and the three droplet sizes. The coverage was measured in the four artificial trees placed in a row, using 26.0 × 76.0 mm water-sensitive papers (WSP) (Syngenta Crop Protection AG, Basel, Switzerland). Twelve WSPs were distributed homogenously on each tree, placed on the *Y-Z* plane that converged with the canopy axis. According to ISO 22,522 standard (ISO, 2007), the canopy was vertically divided into four equal levels: bottom (A), medium low (B), medium high (C), and top (D) (Fig. 7). While the canopy depth was horizontally divided into three equal parts: external left (I), center (II), and external right (III). For each test, both faces of the canopy were sprayed using the same sprayer side. This procedure simulated a common application: the sprayer is driven through a certain row and goes back for the adjacent row, spraying one row with the same sprayer side.

Once dried, the WSPs were collected after every test. They were placed in a plastic folder and stored in a dark container. The described test setup foreseen the use of 12 WSPs per tree, resulting in 48 WSPs per

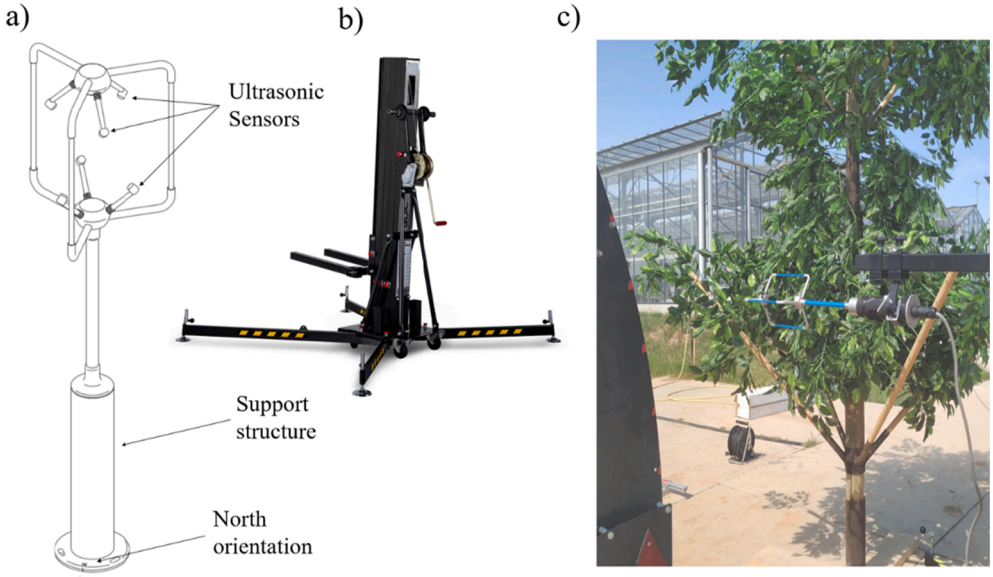

Fig. 5. (a) Schematic view of the 3-axis ultrasonic anemometer, (b) lifting steel device and (c) the anemometer held by the lifting steel device, placed between sprayer outlet and the artificial canopy.

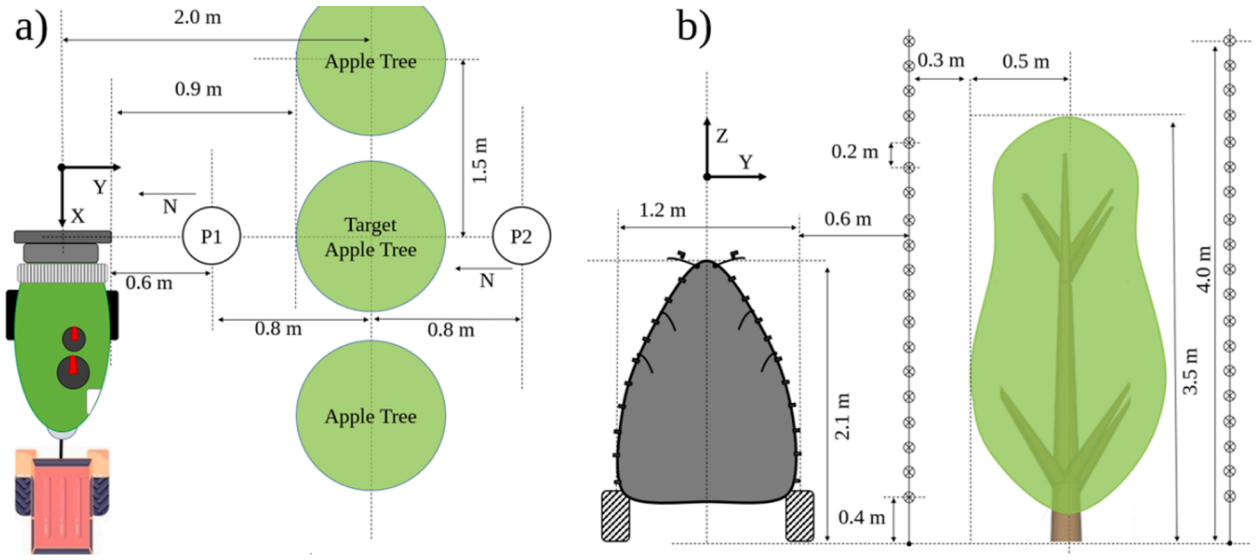

Fig. 6. (a) Schematic plan view of the sprayer emplacement and measuring positions during the static tests, and (b) right schematic elevation view of the sprayer emplacement and the measuring heights during the trials.

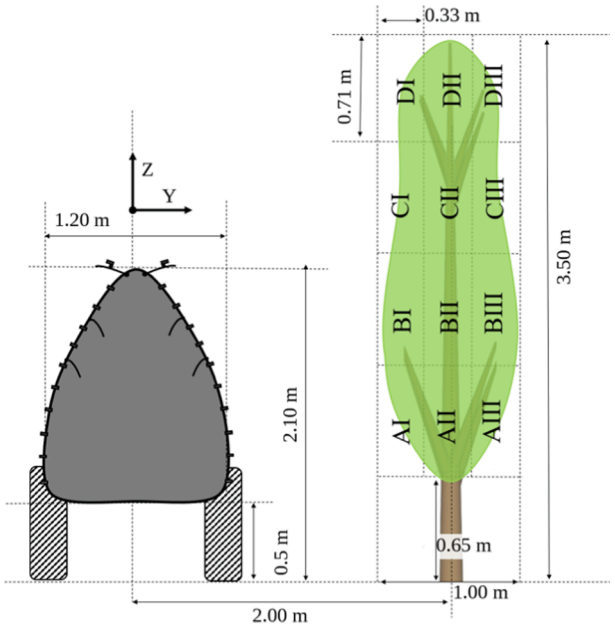

Fig. 7. Scaled scheme of artificial tree segmentation during coverage test. The water sensitive papers (WSP) were placed at twelve positions (four heights and three depths) in four target trees.

test (12 WSPs × 4 trees). In total 1,440 WSP were used (3 nozzle configurations × 5 fan settings × 2 sprayer sides × 48 WSP per test).

2.6. Weather conditions

The environmental wind velocity (direction and magnitude), the temperature, and the relative humidity (RH) were recorded during both trials. The meteorological station was placed 2.0 m above the ground and 25.0 m away from the sprayer. The data was taken at 1.0 Hz using an Hortimax Clima 500 weather station (DS Hortitrade, Netherlands). The main reason to take this data was to guarantee the limits established by the Spanish national legislation in terms of air velocity (<3.0 m s^{-1}) during spray applications (BOE, 2012).

2.7. Data processing

2.7.1. Airflow rate

The airflow velocities obtained from the propeller anemometer were used to estimate the airflow rate in the outlet using the Eq. (1):

$$Q_{Side} = \sum_{i=1}^{33} A_i \times V_i \quad (1)$$

where Q_{side} is the airflow rate expelled (m^3 s^{-1}) per each sprayer side and configuration; A_i represents one sub-area from the outlet surface (m^2); and V_i is the air velocity (m s^{-1}) measured in A_i.

2.8. Air velocities interacting with the canopy

An evaluation to check if the airflow reached a quasi-steady flow was to make sure the air stream obtained is representative (Salcedo et al., 2015, 2019, and 2021). Thus, for each height the cumulative mean for the whole dataset (60.0 s) was computed and studied. If the air velocities in range 30.0 – 60.0 s had standard deviation higher than 5.0 %, then data would not be considered.

The air mean velocity U (m s^{-1}) in each sample location, was calculated for each axis component (U_x, U_y, U_z). Then the magnitude U_T (m s^{-1}) corresponding to each height was obtained using Eq. (2):

$$U_T = \sqrt{U_x^2 + U_y^2 + U_z^2} \quad (2)$$

The fluctuation of the air velocities u' (m s^{-1}) can be defined as the relation between the anemometer measurements, namely instantaneous velocity u (m s^{-1}), and the air mean velocity of each component (Eq. (3)):

$$u' = u - U \quad (3)$$

This fluctuation represents how the instantaneous velocity differs from the mean and it was used to compute the turbulence intensity, I (%). Assuming an isotropic behavior, which meant that the air velocities variations in all direction are similar among them, the fluctuation can be expressed by using the Eq. (4):

$$u_T' = \sqrt{\frac{1}{3}\left(u_x'^2 + u_y'^2 + u_z'^2\right)} \quad (4)$$

where u'_x, u'_y and u'_z (m s^{-1}) are the fluctuation on each axis; and u'_T (m s^{-1}) is the total fluctuation, composed by the three-axes values.

Turbulence intensity quantifies the relation of air velocity fluctuations over the magnitude of the air mean velocity (Eq. (5)). A theoretical airflow without fluctuations would have a turbulence intensity equal to 0.0 %.

$$I(\%) = \frac{u_T^{'}}{U_T} \times 100 \quad (5)$$

Moreover, to characterize the resistance that the canopy presented to the airflow, the drag coefficient C_d was calculated (Da Silva et al., 2006) using Eq. (6):

$$C_d = \frac{1}{\alpha L} \times \ln\left(\frac{U_{Y\_P1}}{U_{Y\_P2}}\right) \quad (6)$$

where α is the leaf area density of each artificial tree, which is 5.3 m2/m^{-3}; U_{Y_P1} and U_{Y_P2} are the mean of all the Y-axis air mean velocities along $P1$ (before the canopy) and $P2$ (behind the canopy), respectively; and L represents the tree depth.

2.8.1. Coverage evaluation

The WSPs were scanned at 600-dpi resolution. Spray coverage was then measured by image processing using ImageJ software (National Institutes of Health, Bethesa, MD, USA). The software estimated the coverage area by filtering the image for different colors between the dry and wet area of the sample. The spray coverage was calculated as the ratio between the spray deposits area and the WSP area. Statistical analysis was performed using the Python module *statsmodel* (Seabold et al., 2010). The dependent variable spray coverage was evaluated by a four-way analysis of variance (ANOVA) with the aim to verify the null hypothesis that all groups within the four independent variables had the same mean: Fan setting, nozzle configuration, sprayer side, and sample position. If the interaction between air configuration and nozzle configuration gave significative differences, another four-way ANOVA was carried out separately for each nozzle type, presenting the coverage as a main factor along four subfactors: air configuration, sprayer side, sample height along the canopy, and sample depth along the canopy. The purpose of this second analysis was to evaluate how changes the significant influence on each nozzle configuration, considering the fan settings and sample position.

3. Results

3.1. Weather conditions

During the tests of the airflow behavior before and after the canopy the average values for the environmental wind speed, temperature and relative humidity were 0.7 m s^{-1}, 13.2 C°, and 80.6 %, respectively. During the coverage trials, the environmental wind speed acquired was 1.5 m s^{-1}, the temperature was 20.6 C°, and the mean relative humidity was at 45.7 %.

3.2. Airflow rate

Table 2 summarizes the air mean velocities, the total airflow rate and its corresponding percentage rate expelled by the two sprayer sides. The configurations A1 and A2, corresponding to the first and second lowest airflow rates, gave almost 50.0 % of the total airflow rate obtained with the other three configurations. The total airflow rate differences between A3 and A5 were<15.0 %. Furthermore, when changing the gearbox position from short to large, the airflow rate increased 5.0 % and 9.0 % for blade pitches 20.0 ° and 35.0 °, respectively. Differently, when the fan gear speed remains fixed, and the blade pitch increased 5.0° (for example, from large 30.0 ° to large 35°), the variation rose up to 15.0 %. Meanwhile, when the blade pitch increased 10.0 ° (for example, from large 20.0 ° to large 30.0 °) the airflow rate increased around 33.0 %. This suggested that the blade pitch had a higher influence on the airflow rate than the fan gearbox position. The largest differences between both sprayers sides were obtained with the fan setting that had the largest airflow rate (A5), the air velocities measured on the right side were 5.0 % larger than the left side. On the other hand, the lowest difference was reached by the medium airflow rate (A3), which the right side expelled 1.0 % more airflow rate than the left side.

All the standard deviations on the left sprayer side were around 40.0 % of the correspondent air mean velocity, while on the right side the standard deviations were around 60.0 % of the mean value. This dispersion was due to the low vertical distribution along the outlet section (Fig. 8). In all configurations the largest air velocities were measured on the bottom part of the outlet. It can be noticed that the left sprayer side increase the heterogeneity as the airflow rate increase. While the right sprayer side presented the lowest homogeneity with the lowest airflow rates (A1 and A2). In addition, on the right side, in heights 100.0 cm to 150.0 cm there were lower airflow rates, and this reduced its homogeneity.

3.3. Airflow behavior before and after the canopy

Fig. 9 shows the components Z and Y of the air mean velocity vectors measured with the 3D-anemometer. The components on the X axis are not presented because in general, they were 1.4 % of the total magnitude. Therefore, the vectors were only represented in the Z-Y plane, containing the main currents. It can be noticed that the right side had air velocities above and before the canopy ($P1$) in all configurations, while

Table 2
Air mean velocities measured on the outlet with the correspondent airflow rate and the percentage rates by sides. The fan settings were sorted by the airflow rate in ascending order. The standard deviation is presented after each value with ±.

Nomenclature	Gearbox position	Blade pitch	Side	Air velocity (m s^{-1})	Airflow rate (m^3 h^{-1})	Percentage rate (%)
A1			Left	9.5 ± 3.4	8,106 ± 87.4	50.7
	Short	20°	Right	9.2 ± 5.5	7,888 ± 143.0	49.3
			Total	9.4 ± 4.6	15,994 ± 118.6	100.0
A2			Left	9.6 ± 4.0	8,247 ± 103.3	49.2
	Large	20°	Right	10.0 ± 6.4	8,514 ± 166.1	50.8
			Total	9.8 ± 5.3	16,761 ± 138.4	100.0
A3			Left	14.7 ± 6.3	12,591 ± 164.4	49.8
	Large	30°	Right	14.8 ± 8.2	12,683 ± 212.7	50.2
			Total	14.8 ± 7.3	25,274 ± 190.1	100.0
A4			Left	16.2 ± 7.6	13,852 ± 197.6	51.0
	Short	35°	Right	15.6 ± 8.5	13,302 ± 219.2	49.0
			Total	15.9 ± 8.1	27,155 ± 208.9	100.0
A5			Left	18.3 ± 8.7	15,633 ± 225.9	52.3
	Large	35°	Right	16.7 ± 9.4	14,252 ± 243.2	47.7
			Total	17.5 ± 9.1	29,885 ± 235.6	100.0

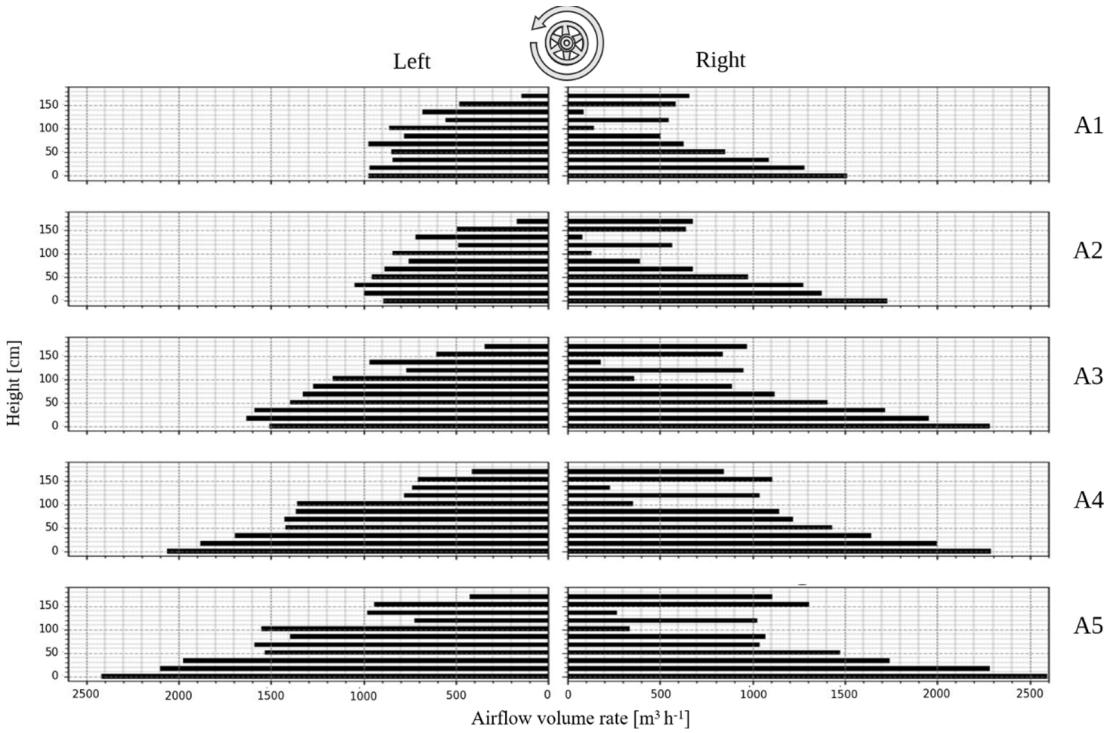

Fig. 8. Vertical profile of the airflow rate estimated from the air velocities measured at the air conveyor outlet. Air configurations stand for the fan settings, sorted by the total airflow rate in ascending order.

the left sprayer side did not. In addition, the vectors measured before the vegetation (*P*1) presented a larger vertical component (pointing the atmosphere) on the right side than the left side. Contrarily, the left sprayer side had bigger air velocity vectors on the bottom part of the canopy than the right sprayer side. This was because the fan rotating sense (counterclockwise) influence, which means an up worth air movement at the right side and a down worth one at the left side. These behaviors coincide with the airflow rate measurements in the outlet section. To analyze the measured air velocities, the sampling heights were divided into three zones: below the canopy (0.4 m – 0.6 m), within the canopy (0.8 m – 3.4 m), and above the canopy (3.6 m – 4.0 m). It was considered that the airflow captured above and below the canopy, as well as the airflow measured after the vegetation, did not transport the droplets to the target canopy. Therefore, they could increase the potential risk of drift contamination.

Table 3 shows the air mean velocity magnitudes and the turbulence intensity, measured within the canopy heights (0.8 m – 3.4 m). It was observed that when changing the gearbox position from short to large and the blade pitch remains fixed, the air velocities increased around 15.0 %. On the other side, when changing the blade pitch from minimum to maximum (20.0 ° to 35.0 °) and the gearbox position remains fixed, the air velocities increased around 50.0 %. This behavior coincided with the results obtained in the airflow rate measurement. Generally, the air velocities measured before the vegetation (*P*1) on the right side were slightly higher than on the left side. The maximum difference between both sides was 20.2 % and it was obtained using the fan setting A4, while the minimum was obtained with the fan setting A5 (11.3 %).

Generally, as larger were the air velocities, lower were the turbulence intensities. Despite of this, the left sprayer side presented larger turbulence intensities than the right side. For example, the air configuration A2 before the canopy had a turbulence intensity of 48.5 % on the left and 21.6 % on the right sprayer side, while the air mean velocities were 4.7 m s^{-1} and 5.6 m s^{-1}, respectively. On the other side, the lowest turbulence intensity before the canopy was obtained when using the right sprayer side and the fan settings that had the largest airflow rate (A5). This combination also had the largest air mean velocity measured after the vegetation (*P*2). This behavior can be seen also in Fig. 9, which shows that a considerable air velocity (up to 8 m s-1) in heights from 1.4 m to 2.0 m, were measured when using the right sprayer side with the air configurations A3, A4, and A5. The left sprayer side on those heights also had an airflow crossing the canopy, but with lower magnitudes.

Fig. 10 presents the relation between the mean intensity turbulence and the drag coefficient. It shows that as higher was the turbulence intensity, larger was the resistance offered by the leaves and branches. Therefore, data suggested that the higher the turbulence intensity, the lower could be the air velocities after the canopy. It could mean that the risk that a fraction of the product could move away beyond the canopy decreased as the turbulence intensity increases.

As shown in Table 4 the air mean velocities measured above and before the vegetation were larger on the right side (>1.5 m s^{-1}) than on the left side (<1.2 m s^{-1}). This confirmed the fan rotation influence, which pushed the airflow on the right sprayer side to the atmosphere, while the airflow in heights 0.4 m and 0.6 m on the left sprayer side tended to go to the ground. Moreover, the largest air velocity above the canopy was obtained when using the right sprayer side with the fan setting that had the medium airflow rate (A3). Therefore, this fan configuration could be the most susceptible to increase the risk of drift. It can be noticed that all the air mean velocities after and above the canopy were below 0.8 m s^{-1}. This meant that the airflow velocities recorded in *P*1 dissipates in the atmosphere before reaching *P*2.

On the other side, the largest air velocities before and below the canopy were obtained when using the medium airflow rate (A3) for both sides. This meant that this configuration could be also the most susceptible to increase the risk of ground loses. Concerning the air velocities measured below and after the canopy, the air configurations that generated the higher air velocities were A5 and A4 for the left and the right side, respectively. In this case (below the canopy), the ground acts as a physical boundary, slowing down the stream action. This is the reason because these air velocities were larger than the ones measured above and after the canopy.

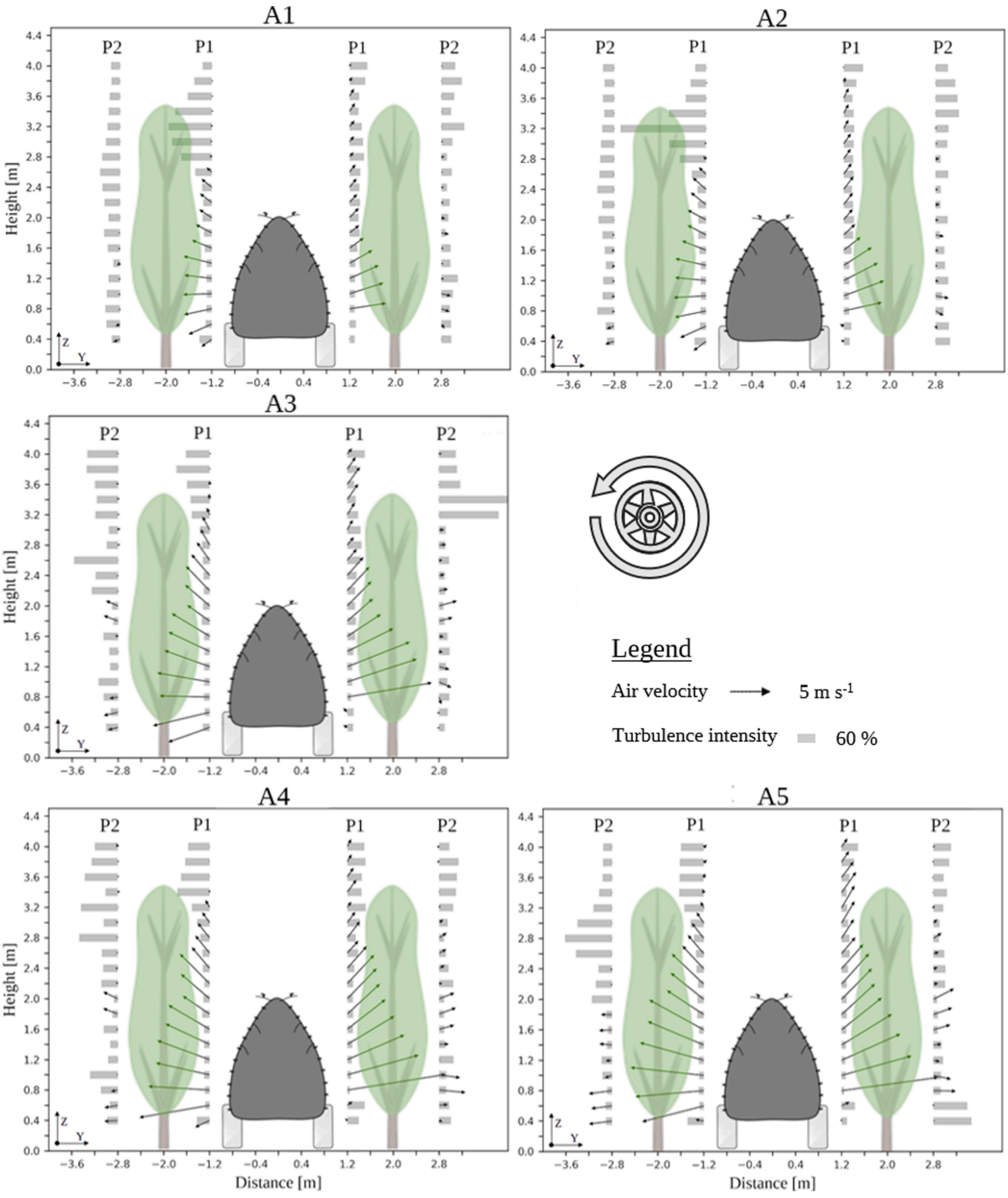

Fig. 9. Air velocity (m/s) vectors computed with Eq. (4) and turbulence intensity I (%) presented with bars, the view is from a rear position of the sprayer. A1 (15,994 m^3/h), A2 (16,761 m^3/h), A3 (25,274 m^3/h), A4 (27,155 m^3/h), and A5 (29,885 m^3/h) stand for the fan settings, sorted by the total airflow rate in ascending order.

Table 3
Mean magnitude of the air velocity vectors within the heights of the canopy (0.8 m – 3.4 m), measured before and after the artificial tree and the correspondent turbulence intensity. The standard deviation is presented after each value with ±.

		Before canopy (*P*1)		After canopy (*P*2)	
Fan setting	Side	Velocity (m s^{-1})	Turbulence intensity (%)	Velocity (m/s)	Turbulence intensity (%)
A1	Left	4.0 ± 2.8	42.9 ± 37.9	0.5 ± 0.2	36.2 ± 8.8
	Right	4.5 ± 2.9	24.0 ± 8.0	1.0 ± 0.7	25.8 ± 12.6
A2	Left	4.7 ± 3.2	48.5 ± 58.6	0.6 ± 0.3	33.0 ± 6.9
	Right	5.6 ± 3.1	21.6 ± 5.3	1.2 ± 0.9	25.5 ± 13.3
A3	Left	8.2 ± 4.1	21.4 ± 11.9	1.3 ± 1.2	43.3 ± 27.4
	Right	9.6 ± 6.4	22.6 ± 8.4	2.1 ± 1.4	19.4 ± 11.8
A4	Left	8.9 ± 4.9	24.2 ± 19.6	1.3 ± 1.3	43.5 ± 27.7
	Right	10.7 ± 6.8	20.6 ± 11.8	2.8 ± 2.0	23.0 ± 11.0
A5	Left	10.6 ± 6.2	23.5 ± 15.9	1.7 ± 1.8	44.4 ± 34.5
	Right	11.8 ± 5.8	14.0 ± 3.9	2.9 ± 2.0	21.4 ± 8.2

Table 4
Mean magnitude of the air velocity vectors above the canopy (3.4 m – 4.0 m) and below the canopy (0.4 m and 0.6 m), measured before and after the artificial tree. The standard deviation is presented after each value with ±.

		Air velocity (m/s)			
		Before canopy (*P*1)		After canopy (*P*2)	
Fan setting	Side	Below	Above	Below	Above
A1	Left	5.1 ± 2.3	0.7 ± 0.1	1.7 ± 0.4	0.5 ± 0.0
	Right	0.8 ± 0.2	1.5 ± 0.8	1.2 ± 0.8	0.5 ± 0.2
A2	Left	5.8 ± 2.3	0.6 ± 0.1	2.3 ± 0.2	0.6 ± 0.1
	Right	1.1 ± 0.3	1.8 ± 1.1	0.9 ± 0.5	0.5 ± 0.1
A3	Left	13.4 ± 2.6	0.8 ± 0.3	3.3 ± 0.8	0.7 ± 0.1
	Right	2.2 ± 1.4	3.9 ± 1.3	0.6 ± 0.0	0.6 ± 0.1
A4	Left	11.6 ± 9.9	0.7 ± 0.0	3.6 ± 0.0	0.7 ± 0.2
	Right	1.7 ± 0.8	2.6 ± 0.4	2.2 ± 0.2	0.7 ± 0.0
A5	Left	9.8 ± 9.8	1.2 ± 0.0	5.8 ± 0.4	0.6 ± 0.0
	Right	1.8 ± 0.3	3.5 ± 1.8	1.3 ± 0.1	0.8 ± 0.3

3.4. Coverage

Several authors haven been considered that a sprayer coverage>30.0 % on the canopy was excessive application and a spray product wasting (Salcedo et al., 2020, Grella et al., 2022b). Considering this threshold, almost all configurations when using the left sprayer side and the fine (T1) or medium (T2) droplet size presented an overspraying application (Table 5). Moreover, the right sprayer side using T1 and the two lowest airflow rates (A1 and A2), also performed an overspraying application. On the other side, the coarser droplet size tended to have the lowest spray coverage as well as the lowest standard deviation. Indeed, the three fan settings A3, A4, and A5 when the coarse droplet size was applied had a mean spray coverage of 25.9 %, 24.1 % and 21.7 %, respectively. While when using the finest droplet size, the spray coverage means were 33.5 %, 39.5 %, and 31.5 % for A3, A4, and A5, respectively. Therefore, it can be noticed that the spray coverage decreased when increasing the droplet size.

Besides this, when A1 and A2 were applied, the spray coverage was greater than when the other three fan settings. This indicates that the spray coverage decreased as increased the airflow rate, being more noticeable as smaller was the droplet size spectra. These results agree with Marucco et al., 2008, which conclude that the upper-leaf deposition decrease as the airflow rate increase.

Table 5
Mean spray coverage (%). The standard deviation is presented after each value with ±.

	F - Fine droplet size		M - Medium droplet size		C - Coarse droplet size	
Fan setting	Left	Right	Left	Right	Left	Right
A1	50.1 ± 24.0	35.3 ± 22.3	46.6 ± 30.3	24.8 ± 12.9	22.7 ± 12.7	34.7 ± 28.4
A2	61.4 ± 23.3	43.9 ± 19.8	40.2 ± 24.1	27.1 ± 14.1	40.8 ± 23.3	23.0 ± 15.9
A3	41.3 ± 21.9	25.7 ± 15.9	35.0 ± 21.0	30.3 ± 13.0	27.5 ± 15.1	24.8 ± 9.5
A4	50.5 ± 17.7	28.5 ± 19.7	42.4 ± 21.2	26.6 ± 18.6	23.4 ± 11.5	24.8 ± 16.8
A5	40.3 ± 16.5	22.7 ± 17.1	26.2 ± 16.8	22.8 ± 14.1	23.1 ± 11.3	20.3 ± 11.2

The spray coverage means when using the left sprayer side were 17.5 %, 11.8 %, and 7.4 % higher, than the spray coverage on right side for fine, medium, and coarse droplet size, respectively. The reason of this spray coverage asymmetry was due to the differences between the air

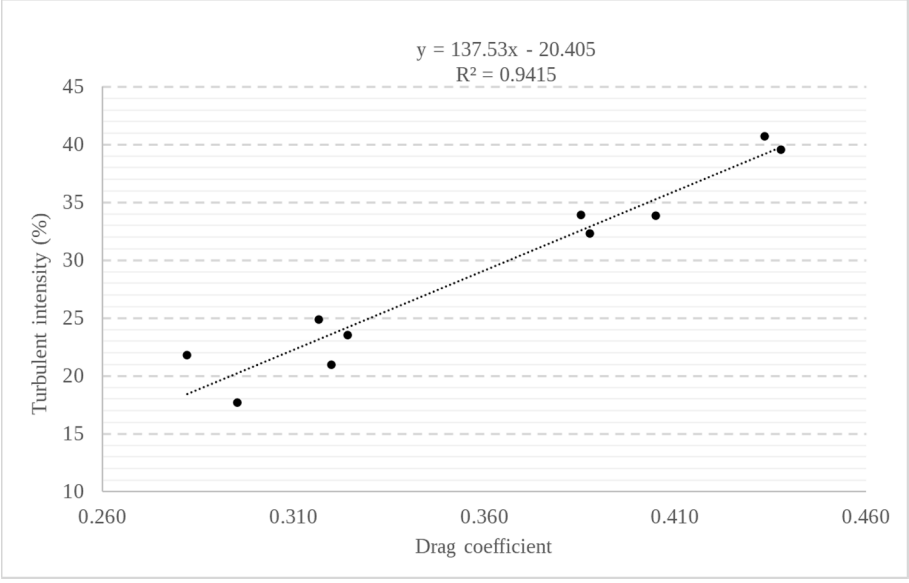

Fig. 10. Relation between turbulence intensity (averaged before and after the canopy) and the drag coefficient computed with Eq. (6).

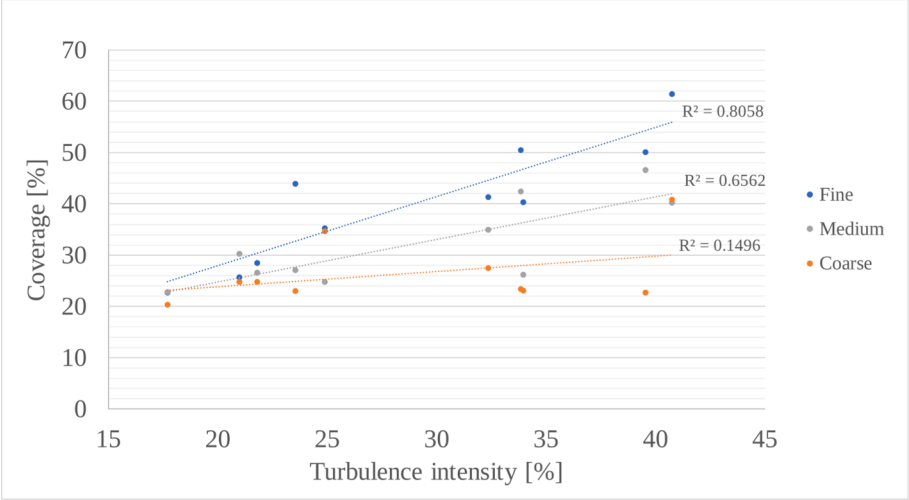

Fig. 11. Relation between turbulence intensity (averaged before and after the canopy) and the spray coverage, for each droplet size.

velocities within the canopy heights. These values indicates that the airflow asymmetry had less influence when the droplet size spectra increased. Moreover, the coarse droplet size presented two air configurations (A2 and A4) which covered more the right side than the left side. In addition, the coarse droplet size when using A3, A4, and A5 had<3p.p. between both sides.

Fig. 11 shows the relation between the spray coverage (Table 5) and the turbulence intensity (Table 3) averaged before and after the vegetation. It can be observed that as the turbulence intensity increased the spray coverage increased. Although this tendency, the coefficient of determination increased as the droplet size decreased, being lower than 0.2 when using the coarse droplet size. Considering that the turbulent intensity decreased with increasing air velocities, these data suggest that the larger the droplet size, the smaller the influence of the airflow on the coverage. However, a larger airflow could have other effects such as greater penetration. Future work is needed to relate different canopy diameters and leaf densities with different nozzle sizes.

To analyze the spray coverage uniformity, Fig. 12 shows the mean for each sample position and configuration. It can be detected spray coverage values above 60.0 % in most of cases when using the left sprayer side. However, these cases also had spray coverage values close to 10.0 %. This reduced the overall uniformity along the canopy. On the other hand, almost all the samples obtained with the three largest airflow rates (A3, A4, and A5) and the coarse droplet size, as well as the medium droplet size on the right side, were below 40.0 %.

It can be noticed that the coarse droplet tended to have larger spray coverage differences in the vertical axis than in the horizontal axis (for example, the fan setting A3 on the left side). In other words, it had a larger uniformity along the horizontal axis than the vertical axis. Furthermore, most cases presented the lowest coverage on the top part of the canopy, meaning that the main difficulty is to transport the droplet size to the top part. Contrarily, when the finest droplet size spectra was applied, potential problems in penetration were noticed. When the left sprayer side was used, most samples taken on the external canopy zones had a spray coverage>50.0 %, while the inner samples showed spray coverage values up to 10.0 %. This behavior reduces the penetration. It can be detected because it generated vertical contour lines in their graphical representations. Concerning the medium droplet size, when using the fan configurations A2 and A3 on the left side, the application had problems in penetration (vertical contour lines). On the other side, when using A1 on the left and right side, the application could have problems on transporting the droplet to the top part of the canopy. Therefore, this nozzle configuration presented both problems discussed on the other two nozzle configuration.

Indeed, the first ANOVA demonstrates that the coverage measured was significantly affected by the four studied parameters: Sprayer side (F-ratio = 15; df = 1; $p < 0.05$); Fan settings (F-ratio = 4; df = 4; $p < 0.05$); Nozzle configuration (F-ratio = 10; df = 2; $p < 0.05$); and sample position along the canopy (F-ratio = 9; df = 11; $p < 0.05$). The interaction between fan setting and sprayer side did not present significance differences (F-ratio = 2; df = 4; $p > 0.05$), this meant that the sprayer side influence on the coverage was independent of the fan setting. The sample position when interacting with the nozzle configuration gave significant changes (F-ratio = 3; df = 22; $p < 0.05$), but not when interacting with air settings (F-ratio = 1; df = 44; $p > 0.05$).

To further analyze this significance, Table 6 shows the results of the four-way ANOVA made by each nozzle type, the spray coverage was the main factor along with four subfactors: fan setting, sample position (height and depth) along the canopy, and sprayer side. The air setting did not present significant influences when using the coarse droplet size, while for the medium and fine droplet size the differences were significant. In addition, the p-value increase as the droplet size increase, which could mean that the significative influence decrease. The same behavior can be observed for the sprayer side influence. This indicates that as larger the droplet size spectra, the less influence had the airflow rate on spray coverage. Contrarily, the sample height presented significant differences when using the medium and coarse droplet size, but not with the finest droplet size. In this case, the p value decreased as the droplet size increase. This meant that the larger the droplet size, the lower vertical homogeneity. On the other side, the samples position in depth had the same significative influence for the three nozzle size. This meant that, probably, the penetration is affected more by the airflow rate than by the nozzle size.

4. Conclusions

This work showed how the fan blade pitch and the gearbox position affected on the airflow rate, air symmetry between both sprayer sides, and canopy resistance to the airflow, as well as the utility of using ultrasonic anemometers to study the air currents effects. When increasing the airflow rate, both turbulence intensity and symmetry between sprayer sides decreased. However, as larger the droplet size and the airflow rate, higher the spray coverage homogeneity.

Experimental data from the anemometer exposed that the larger the turbulence intensity the higher the resistance offered the canopy to the airflow, which meant that the gradient of air velocities before and after the canopy increased. In addition, as larger the turbulence intensity, higher spray coverage was obtained. Even so, the droplet size was critical on regulating the airflow influence on spray coverage, as larger the droplet size, the less influence had the air velocities and its turbulence

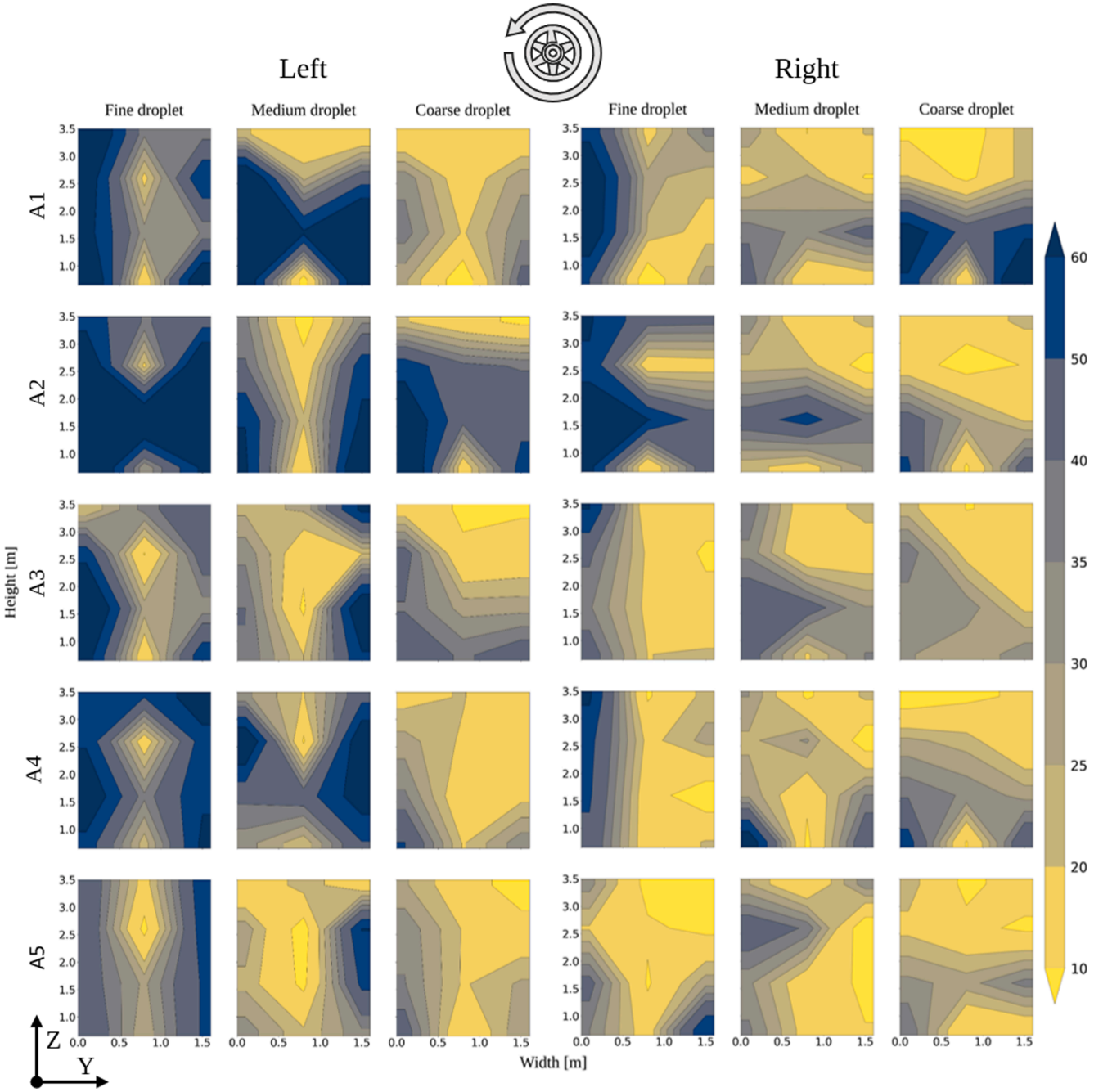

Fig. 12. Canopy coverage map, color levels go from 10.0 % spray coverage, painted in yellow (minimum) to 60.0 % spray coverage, painted in blue (maximum). A1 (15,994 m^3/h), A2 (16,761 m^3/h), A3 (25,274 m^3/h), A4 (27,155 m^3/h), and A5 (29,885 m^3/h) stand for the fan settings, sorted by the total airflow rate in ascending order.

Table 6
Results of the four-way ANOVA (95.0 % confidence level) for the sprayer coverage. Each nozzle configuration was analyzed separately.

		Coverage (%)					
		F – Fine Droplet		M – Medium Droplet		C – Coarse Droplet	
	DF	p > (F)	Sign.	p > (F)	Sign.	p > (F)	Sign.
Main effects							
Air Setting	4	9.65 E-07	***	1.59 E-03	**	5.09 E-02	NS
Height	3	1.51 E-01	NS	9.22 E-07	***	1.18 E-18	***
Depth	2	3.22 E-27	***	1.46 E-15	***	2.79 E-13	***
Sprayer side	1	1.10 E-14	***	4.85 E-09	***	1.07 E-01	NS
Interactions							
Air setting × Height	12	2.11 E-01	NS	1.72 E-02	*	5.58 E-01	NS
Air setting × Depth	8	1.63 E-01	NS	6.65 E-01	NS	1.19 E-02	*
Height × Depth	6	6.62 E-03	**	2.81 E-02	*	3.35 E-06	**
Sprayer side × Air setting	4	7.70 E-01	NS	9.74 E-02	NS	8.47 E-04	***
Sprayer side × Height	3	8.81 E-01	NS	1.90 E-01	NS	7.33 E-02	NS
Sprayer side × Depth	2	1.46 E-05	***	1.48 E-10	***	2.14 E-01	NS

Statistical significance level: NS stands for values of $p > 0.05$; * stands for values of $0.05 > p > 0.01$; ** stands for values of $0.01 > p > 0.001$; *** stands for values of $p < 0.001$.

on the spray coverage. The coarse droplet size seemed that it was presenting a very low dependency on the fan settings. On the other side, the finest droplet size was more under the influence of the airflow.

This work showed how the fan settings influence on the nozzle selection to adjust the spray coverage. However, further test to study the turbulence intensity, air velocities and spray coverage, by using ultrasonic anemometers and processing image softwares, are needed to understand their interdependency.

CRediT authorship contribution statement

Bernat Salas: Investigation, Methodology, Writing – original draft. **Ramón Salcedo:** Conceptualization, Methodology, Writing – review & editing, Writing – original draft. **Paula Ortega:** Investigation, Data curation, Writing – review & editing. **Marco Grella:** Methodology, Data curation, Writing – review & editing. **Emilio Gil:** Conceptualization, Resources, Writing – review & editing, Supervision.

Declaration of Competing Interest

The authors declare that they have no known competing financial interests or personal relationships that could have appeared to influence the work reported in this paper.

Data availability

Data will be made available on request.

Acknowledgements

This project has received funding from the European Union's Horizon 2020 research and innovation program under grant agreement No 773718 (OPTimised Integrated pest Management for precise detection and control of plant diseases in perennial crops and open-field vegetables, www.optima-h2020.eu). Bernat Salas received funding for his Ph. D. development from Agència de Gestió D'Ajuts Universitaris I de Recerca (AGAUR) (file N° FI_B 01193).

The authors would like to express their appreciation to Dr. David Nuyttens, ILVO (Belgium), for his support in measuring the droplet size for classification of nozzles.

References

ASABE S572.3, 2020. Spray nozzle classification by drop spectra. American Society of Agricultural and Biological Engineers.

Baldoin, C., Amistà, F., Beria, S., Zelante, A., 2001. Quality of distribution, drift and ground losses from four low-volume orchard sprayers on apple. Parasitica 57, e125.

Balsari, P., Gil, E., Marucco, P., van de Zande, J.C., Nuyttens, D., Herbst, A., Gallart, M., 2017. Field-crop-sprayer potential drift measured using test bench: Effects of boom height and nozzle type. Biosyst. Eng. 154, 3–13. https://doi.org/10.1016/j.biosystemseng.2016.10.015.

Benbrook, C.M., Baker, B.P., 2014. Perspective on dietary risk assessment of pesticide residues in organic food. Sustainability 6, 3552–3570. https://doi.org/10.3390/su6063552.

Berger, L.T., Ortega, P., Gil, E., 2019. Smartomizer – proactivity and traceability in orchard spraying. In: 15th Workshop on Spray Application and Precision Technology in Fruit Growing Programme and Abstracts, p. 43.

BOE (Boletín Oficial del Estado), 2012. Real Decreto 1311/2012, de 14 de septiembre, por el que se establece el marco de actuación para conseguir un uso sostenible de los productos fitosanitarios. BOE N 223 de 15 de septiembre, 65127–65171.

Carvalho, F.P., 2017. Pesticides, environment, and food safety. Food Energy Secur. 6 (2), 48–60. https://doi.org/10.1002/fes3.108.

European Commission, 2019. Communication from the commmission to the european parliament, the european council, the council, the european economic and social commmittee and the commmittee of the regions, the european green deal. European Commission: Brussels, Belgium.

European Commission, 2020a. Communication from the commmission to the european parliament, the european council, the council, the european economic and social commmittee and the commmittee of the regions, farm to fork strategy for a fair, healthy and environmentally-friendly food system. European Commission: Brussels, Belgium.

European Commission, 2020b. Communication from the commission to the european parliament, the council, the european economic and social committee and the committee of the regions, eu biodiversity strategy for 2030. European Commission: Brussels, Belgium.

Da Silva, A., Sinfort, C., Tinet, C., Pierrat, D., Huberson, S., 2006. A Lagrangian model for spray behaviour within vine canopies. Aerosol Sci. 37 (5), 658–674. https://doi.org/10.1016/j.jaerosci.2005.05.016.

Dekeyser, D., Duga, A.T., Verboven, P., Endalew, A.M., Hendrickx, N., Nuyttens, D., 2013. Assessment of orchard sprayers using laboratory experiments and computational fluid dynamics modelling. Biosyst. Eng. 114 (2), 157–169. https://doi.org/10.1016/j.biosystemseng.2012.11.013.

Dekeyser, D., Foqué, D., Duga, A.T., Verboven, P., Hendrickx, N., Nuyttens, D., 2014. Spray deposition assessment using different application techniques in artificial orchard trees. Crop Prot. 64, 187–197. https://doi.org/10.1016/j.cropro.2014.06.008.

Delele, M.A., Jaeken, P., Debaer, C., Baetens, K., Endalew, A.M., Ramon, H., Nicolaï, B. M., Verboven, P., 2007. CFD prototyping of an air-assisted orchard sprayer aimed at drift reduction. Comput. Electron. Agric. 55 (1), 16–27. https://doi.org/10.1016/j.compag.2006.11.002.

Doruchowski, G., Świechowski, W., Masny, S., Maciesiak, A., Tartanus, M., Bryk, H., Hołownicki, R., 2017. Low-drift nozzles vs. standard nozzles for pesticide application in the biological efficacy trials of pesticides in apple pest and disease control. Sci. Total Environ. 575, 1239–1246. https://doi.org/10.1016/j.scitotenv.2016.09.200.

Ferguson, J.C., O'Donnell, C.C., Chauhan, B.S., Adkins, S.W., Kruger, G.R., Wang, R., Ferreira, P.H.U., Hewitt, A.J., 2015. Determining the uniformity and consistency of droplet size across spray drift reducing nozzles in a wind tunnel. Crop Prot. 76, 1–6. https://doi.org/10.1016/j.cropro.2015.06.008.

Gaona, L., Bedmar, F., Gianelli, V., Faberi, A.J., Angelini, H., 2019. Estimating the risk of groundwater contamination and environmental impact of pesticides in an agricultural basin in Argentina. Environ. Sci. Technol. 16 (11), 6657–6670. https://doi.org/10.1007/s13762-019-02267-w.

Garcera, C., Molto, E., Chueca, P., 2017. Spray pesticide applications in Mediterranean citrus orchards: Canopy deposition and off-target losses. Sci. Total Environ. 599, 1344–1362. https://doi.org/10.1016/j.scitotenv.2017.05.029.

Garcera, C., Moltó, E., Izquierdo, H., Balsari, P., Marucco, P., Grella, M., Gioelli, F., Chueca, P., 2022. Effect of the Airblast Settings on the Vertical Spray Profile:

Implementation on an On-Line Decision Aid for Citrus Treatments. Agronomy 12, 1462. https://doi.org/10.3390/agronomy12061462.
García-Ramos, F.J., Serreta, A., Boné, A., Vidal, M., 2018. Applicability of a 3D Laser Scanner for Characterizing the Spray Distribution Pattern of an Air-Assisted Sprayer. J. Sens. 2018, 1–7.
Gil, E., Llorens, J., Landers, A., Llop, J., Giralt, L., 2011. Field validation of Dosaviña, a decision support system to determine the optimal volume rate for pesticide application in vineyards. Eur. J. Agron. 35 (1), 33–46. https://doi.org/10.1016/j.eja.2011.03.005.
Gil, E., Landers, A., Gallart, M., Llorens, J., 2013. Development of two portable patternators to improve drift control and operator training in the operation of vineyard sprayers. Spanish J. Agric. Res. 11, 615–625. https://doi.org/10.5424/sjar/2013113-3638.
Gil, E., Balsari, P., Gallart, M., Llorens, J., Marucco, P., Andersen, P.G., Fàbregas, X., Llop, J., 2014. Determination of drift potential of different flat fan nozzles on a boom sprayer using a test bench. Crop Prot. 56, 58–68. https://doi.org/10.1016/j.cropro.2013.10.018.
Gil, E., Ortega, P., Salas, B., Andreu, F., Berger, L.T., Fountas, S., Nuyttens, D., 2020. Development of a methodology to select the optimal application technologies in apple crop–EU project OPTIMA-H2020. Assoc. Appl. Biol. 67–75.
Grella, M., Gallart, M., Marucco, P., Balsari, P., Gil, E., 2017. Ground deposition and airborne spray drift assessment in vineyard and orchard: The influence of environmental variables and sprayer settings. Sustainability 9 (5), 728. https://doi.org/10.3390/su9050728.
Grella, M., Marucco, P., Zwertvaegher, I., Gioelli, F., Bozzer, C., Biglia, A., Manzone, M., Caffini, A., Fountas, S., Nuyttens, D., Balsari, P., 2022a. The effect of fan setting, air-conveyor orientation and nozzle configuration on airblast sprayer efficiency: Insights relevant to trellised vineyards. Crop Prot. 155, 105921. https://doi.org/10.1016/j.cropro.2022.105921.
Grella, M., Gioelli, F., Marucco, P., Zwertvaegher, I., Mozzanini, E., Mylonas, N., Nuyttens, D., Balsari, P., 2022b. Field assessment of a pulse width modulation (PWM) spray system applying different spray volumes: duty cycle and forward speed effects on vines spray coverage. Precis. Agric. 23, 219–252. https://doi.org/10.1007/s11119-021-09835-6.
Hilz, E., Vermeer, A.W.P., 2013. Spray drift review: The extent to which a formulation can contribute to spray drift reduction. Crop Prot. 44, 75–83. https://doi.org/10.1016/j.cropro.2012.10.020.
Hong, S.W., Zhao, L., Zhu, H., 2018. CFD simulation of pesticide spray from air-assisted sprayers in an apple orchard: Tree deposition and off-target losses. Atmos. Environ. 175, 109–119. https://doi.org/10.1016/j.atmosenv.2017.12.001.
ISO 22522, 2007. Crop Protection Equipment e Field Measurement of Spray Distribution in Tree and Bush Crops. International Standards Organization.
ISO 22866, 2005. Equipment for crop protection. Methods for field measurements of spray drift. International Standards Organization.
ISO 25358, 2018. Crop Protection, Droplet-size spectra from atomizers - Measurement and classification. International Standards Organization.
ISO 9898, 2000. Equipment for crop protection. Test methods for air-assisted sprayers for bush and trees. International Standards Organization.
Marucco, P., Tamagnone, M., Balsari, P., 2008. Study of air velocity adjustment to maximise spray deposition in peach orchards. Agric. Eng. Int. CIGR J. 1–13. http://www.cigrjournal.org/index.php/Ejounral/article/viewFile/1252/1109.
Marucco, P., Balsari, P., Grella, M., Pugliese, M., Eberle, D., Gil, E., Llop, J., Fountas, S., Mylonas, N., Tsitsigiannis, D., Balafoutis, A., Polder, G., Nuyttens, D., Dias, L., Douzals, J.P., 2019. OPTIMA EU project: Main goal and first results of inventory of current spray practices in vineyards and orchards. In: in 15th Workshop on Spray Application and Precision Technology in Fruit Growing Programme and Abstracts, p. 99.
McCoy, M.L., Hoheisel, G.-A., Khot, L.R., Moyer, M.M., 2022. Adjusting air-assistance and nozzle style for optimized airblast sprayer use in eastern washington vineyards. Catalyst: Discovery into. Practice 6, 9–19. https://doi.org/10.5344/catalyst.2021.21001.
Miranda-Fuentes, A., Rodríguez-Lizana, A., Gil, E., Agüera-Vega, J., Gil-Ribes, J.A., 2015a. Influence of liquid-volume and airflow rates on spray application quality and homogeneity in super-intensive olive tree canopies. Sci. Total Environ. 537, 250–259. https://doi.org/10.1016/j.scitotenv.2015.08.012.
Miranda-Fuentes, A., Gamarra-Diezma, J.L., Blanco-Roldán, G.L., Cuenca, A., Llorens, J., Rodríguez-Lizana, A., Gil, E., Agüera-Vega, J., Gil-Ribes, J.A., 2015b. Testing the influence of the airflow rate on spray deposit, coverage and losses to the ground in a super-intensive olive orchard in southern Spain. In: 13th Workshop on Spray Application in Fruit Growing, pp. 17–18.
Miranda-Fuentes, A., Marucco, P., González-Sánchez, E.J., Gil, E., Grella, M., Balsari, P., 2018. Developing strategies to reduce spray drift in pneumatic spraying in vineyards: Assessment of the parameters affecting droplet size in pneumatic spraying. Sci. Total Environ. 616–617, 805–815. https://doi.org/10.1016/j.scitotenv.2017.10.242.
Musiu, E.M., Qi, L., Wu, Y., 2019. Spray deposition and distribution on the targets and losses to the ground as affected by application volume rate, airflow rate and target position. Crop Prot. 116, 170–180. https://doi.org/10.1016/j.cropro.2018.10.019.
Nuyttens, D., Baetens, K., De Schampheleire, M., Sonck, B., 2007b. Effect of nozzle type, size and pressure on spray droplet characteristics. Biosyst. Eng. 97, 333–345. https://doi.org/10.1016/j.biosystemseng.2007.03.001.
Nuyttens, D., Schampheleire, M. De, Baetens, K., Sonck, B., 2007. The influence of operator-controlled variables on spray drift from field crop sprayers. Trans. ASABE, 50, 1129–1140. 10.13031/2013.23622.
Optima, 2019. Optimised Pest Integrated Management to precisely detect and control plant diseases in perennial crops and open-field vegetables. Horizon 2020, 773718. https://cordis.europa.eu/project/id/773718/es.
European Parliament, 2009. Directive 2009/128/ec of the european parliament and of the council of 21 october 2009 establishing a framework for community action to achieve the sustainable use of pesticides. 2009/128/EC.
Pascuzzi, S., Cerruto, E., Manetto, G., 2017. Foliar spray deposition in a "tendone" vineyard as affected by airflow rate, volume rate and vegetative development. Crop Prot. 91, 34–48. https://doi.org/10.1016/j.cropro.2016.09.009.
Fox, R. D., Derksen, R. C., Zhu, H., Brazee, R. D., Svensson, S. A., 2008. A history of air-blast sprayer development and future prospects. Trans. ASABE, 51, 405–410. 10.13031/2013.24375.
Salcedo, R., Garcera, C., Granell, R., Molto, E., Chueca, P., 2015. Description of the airflow produced by an air-assisted sprayer during pesticide applications to citrus. Spanish J. Agric. Res. 13, 1–15. https://doi.org/10.5424/sjar/2015132-6567.
Salcedo, R., Vallet, A., Granell, R., Garcerá, C., Moltó, E., Chueca, P., 2017. Eulerian-Lagrangian model of the behaviour of droplets produced by an air-assisted sprayer in a citrus orchard. Biosyst. Eng. 154, 76–91. https://doi.org/10.1016/j.biosystemseng.2016.09.001.
Salcedo, R., Pons, P., Llop, J., Zaragoza, T., Campos, J., Ortega, P., Gil, E., 2019. Dynamic evaluation of airflow stream generated by a reverse system of an axial fan sprayer using 3D-ultrasonic anemometers. Effect of canopy structure. Comput. Electron. Agric. 163, 104851 https://doi.org/10.1016/j.compag.2019.06.006.
Salcedo, R., Zhu, H., Zhang, Z., Wei, Z., Chen, L., Ozkan, E., Falchieri, D., 2020. Foliar deposition and coverage on young apple trees with PWM-controlled spray systems. Comput. Electron. Agric. 178, 105794 https://doi.org/10.1016/j.compag.2020.105794.
Salcedo, R., Fonte, A., Grella, M., Garcerá, C., Chueca, P., 2021. Blade pitch and air-outlet width effects on the airflow generated by an airblast sprayer with wireless remote-controlled axial fan. Comput. Electron. Agric. 190 https://doi.org/10.1016/j.compag.2021.106428.
Sankhla, M. S., 2018. Water Contamination through pesticide & their toxic effect on human health. Int. J. Res. Appl. Sci. Eng. Technol. 6, 967–970. 10.22214/ijraset.2018.1146.
Schäfer, R.B., Liess, M., Altenburger, R., Filser, J., Hollert, H., Roß-Nickoll, M., Schäfer, A., Scheringer, M., 2019. Future pesticide risk assessment: narrowing the gap between intention and reality. Environ. Sci. Eur. 31 (1), 1–5. https://doi.org/10.1186/s12302-019-0203-3.
Seabold, S., Perktold, J., 2010. Statsmodels: Econometric and statistical modeling with Python. Proceedings of the 9th Python in Science Conference, (Scipy), 92–96. 10.25080/majora-92bf1922-011.
Sultana, P., Testuyuki, K., Moloy, B., Nobukazu, N., 2005. Predicting herbicides concentrations in paddy water and runoff to the river basin. Environm. Sci. 17, 631–636.
Tilman, D., Balzer, C., Hill, J., Befort, B. L., 2011 Global food demand and the sustainable intensification of agriculture. Proc. Nat. Acad. Sci. 108, 20260–20264. 10.1073/pnas.1116437108.
Van de Zande, J.C., Stallinga, H., Michielsen, J.M.G.P., van Velde, P., 2005. Effect of sprayer speed on spray drift. Ann. Rev. Agric. Eng. 4 (1), 129–142.
Xiahou, B., Sun, D., Song, S., Xue, X., Dai, Q., 2020. Simulation and experimental research on droplet flow characteristics and deposition in airflow field. Int. J. Agric. Biol. Eng. 13 (6), 16–24. https://doi.org/10.25165/j.ijabe.20201306.5455.
Xun, L., García-Ruiz, F., Fàbregas, X., Gil, E., 2022. Pesticide dose based on canopy characteristics in apple trees: Reducing environmental risk by reducing the amount of pesticide while maintaining pest and disease control efficacy. Sci. Total Environ. 826, 154204 https://doi.org/10.1016/j.scitotenv.2022.154204.
Zhou, Y., Mengmeng, N., Jun, L., Xing, X., Jitong, X., Zhaochun, C., 2015. Design and experiment of an electrostatic sprayer with online mixing system for orchard. Trans. Chinese Soc. Agric. Eng. 31 (21), 60–67.